A Demonstration of Precise Calibration of Tropospheric Delay Fluctuations with Water Vapor Radiometers

1,.1'. Teitelbaum, S.J. Keihm, R.P. Linfield, M.J. Mahoney, and G.M. Resch
Jet I 'repulsion Laboratory, California Institute of Technology, Pasadena

Received RECEIPT DATE; revised REVISION DATE; accepted ACCEPTANCE DATE.

To appear in the *Geophysical Research Letters*, 1996.

Short title: TROPOSPHERE CALIBRATION

Abstract. The ability of Water Vapor Radiometers (WVRs) to calibrate changes in tropospheric delay was demonstrated during very long baseline radio interferometer (VLBI) observations at Goldstone, California. WVR measurements reduced the observed VLBI delay variations over a 13 hr period by a factor of ≈ 2.5. When applied to shorter time scales, a ≈ 500/0 reduction in 100- 700 s delay variations was achieved during conditions of high tropospheric activity. Thermal WVR noise precluded calibration of short time scale delay fluctuations during quiet tropospheric conditions.

Introduction

The main objective of a Very Long Baseline Interferometry (VLBI) observation of a compact natural radio source or a Doppler tracking measurement of a spacecraft, is to estimate the *geometric* delay or delay rate, respectively, from which the angular position of the source on the sky or the radial velocity of the spacecraft can be accurately determined. The geometric delay/delay rate is the delay/delay rate which would be measured if perfect instrumentation detected signals traveling through vacuum between the signal source and the Earth. Radio science experiments infer phenomena of physical interest, for example, the structure of a planetary atmosphere or evidence for the passage of a gravitational wave, by measuring perturbations to the geometric delay/clclay rate along a spacecraft tracking link. However, non-geometric effects which corrupt the *measured* delay/delay rate must first be removed from the data, either by modeling ant] estimation or by direct calibration. For measurements that arc insensitive to the effects of ionized media, such as high single frequency ($\nu \gtrsim 20$ GHz) Doppler or dual frequency VLBI, non-dispersive tropospheric effects will dominate the media contribution to the signal. Although a mean tropospheric delay can be estimated from the data, stochastic tropospheric fluctuations shout the mean have substantial power over a wide range of time scales [*Treuhaft* and *Lanyi,* 1987].

Measurements at 32 GHz of the two-way phase between Earth and the Cassini spacecraft during its cruise to Saturn will be used to search for low frequency (10^{-4} to 10--2 Hz) gravitational radiation. The sensitivity of the search will be limited by our ability to calibrate the tropospheric delay on the uplink and downl ink signals. Because most of the power in tropospheric delay fluctuations at frequencies <0.01 Hz is believed to be clue to fluctuations in water vapor density [*Hinder,* 1970], efforts at calibrating these *wet* delay fluctuations have focused on the usc of Water Vapor Radiometers (WVRs) [*Elgered,* 1993].

A short baseline VLBI experiment isolates wet delay fluctuations because most

delay errors cancel or are negligible on baselines $\lesssim$ 200 km. The VLBI delay residuals (i. c., after subtraction of an accurate model) will be dominated by unmodeled delay variations in the wet troposphere. A previous attempt to calibrate delay fluctuations with WVRs [*Linfield et al.*, 1996] was only marginally successful, due to quiet tropospheric conditions and difficulties with instrumentation at one radio antenna. However, the present experiment convincingly demonstrates the ability of current generation WVRs to precisely measure short time scale path delay fluctuations and to provide a calibration which dramatically reduces the impact of unmodeled, tropospheric delay variations on VLBI observations.

Observations and Data Reduction

On Sept. 10 11, 1994 at Goldstone, California, wc conducted dual frequency (2.3 and 8.4 GHz) VLBI observations on the 21 km baseline between two of NASA's Deep Space Network (DSN) 34 m diameter antennas: a new beam waveguide antenna at DSS13 and a high efficiency antenna at DSS15. in order to reduce tropospheric sampling differences duc to beam offset, WVRs [*Janssen 1985, Keihm, 1991*] were positioned approximately 50 m from each DSN antenna, the minimum separation that still allowed a clear WVR. field of view. These short baseline measurements took place during an intercontinental VLBI experiment. Wc inherited a schedule optimized for astrometry, including frequent low elevation angle measurements clown to the VLBI horizon at $\theta = 6°$. Because the WVRs had large conical beams of $\sim 6 - 9°$ (FWHM) a WVR horizon was imposed at $\theta = 30°$ to avoid ground pickup. The WVRs do not track sidereally and were pointed at the mean elevation and azimuth angles during each scan.

'1'here were 175 scans, spanning 15 hours. All scans were 110-160 s long, except for three long scans that were $\approx$ 2000 s in length. The long scans were scheduled at high elevations angles $\theta > 40°$ which assured that WVR co-pointing was possible. They were also timed to occur near source meridian transit, which minimized changes in elevation

angle during the **scans.** These would introduce systematic delay trends in the VLBI data, due to changing path length through the mean troposphere. This experimental setup was nearly identical to that in our previous observations [*Linfield et al., 1996*]. Weather conditions were warm and clear.

Formatted data streams from both DSN antennas were cross-correlated in real time. The correlator output was processed with astrometric and geodetic data reduction software. Fringe fitting estimated onc group delay and phase delay rate for each scan, for each of the two frequency bands, and a time series of interferometer residual phases with respect to the fitted model. Bright, sources were selected for the long scans so that a precise residual phase could be extracted every 2 s. A linear combination of the observables from each frequency band was formed; this removed the effect of charged particles in the ionosphere and interplanetary medium. The charged partic]c-free group delays were used as input observables to a multiparameter estimation step which extracted model parameters. The scan-to-scan residuals with respect to the model are expected to be dominated by unmodeled tropospheric fluctuations about the average, site-dif~crcnccc], zenith troposphere estimated from the data.

W VR output voltages were converted to brightness temperatures using gains estimated by the tip curve method. Brightness temperatures were converted to path delays using linear retrieval coefficients determined from model calculations based on radiosonde data. Although both WVRs were two-channel instruments, all results reported here used only the lower noise, vapor- sensing channel at 20.7 GHz, sufficient under the clear conditions of our observations. A line-of-sight (LOS) path delay was estimated for each WVR every ~ 6 s. A number of scans were lost to data acquisition failures of either the VLBI or WVRs. Scans were also rejected if the WVR brightness tempera.turcs exhibited evidence of ground pickup or contamination from radio emission from the sun, or if the VLBI post-fit residuals were clear outliers in the full experiment solution. The full, valid data set consisted of 80 scans. When the WVRS were forced to

point at higher elevation angles θ_W than the DSN antennas, estimates of the 1,0S delays were determined by assuming that LOS path delays $\tau(0)$ were related to WVR-derived path delays $\tau_W(O_w)$ by the mapping function $\tau(0) = \tau_W(\theta_W) \sin \theta_W / \sin \theta$. A subset of the valid data for which the WVR and VLBI antennas were co-pointed to within 1° at both ends of the baseline consisted of 30 scans. A more detailed description of the data reduction can be found in [*Linfield et al., 1996*].

Results and Discussion

The time series of the site-differenced (DSS13- DSS15) 1,0S delay residuals for two long scans for the VLBI and WVR data arc shown in Figure 1. The VLBI delays τ arc determined every two seconds from the measured interferometer residual phase. A linear trend has been subtracted from the VLBI data during fringe fitting [*Lowe* 1992], removing any clock-like effects. To insure comparable treatment of the WVR data, the path delay time series of each WVR has had an equivalent linear model estimated and removed. This is important because at a fixed elevation angle a site- differenced, tropospheric delay which varies linearly wit h time is indist inguishable from a linearly-drifting clock. Because both the time-tagging and the data acquisition duty cycles are different for each WVR, the WVR residual delays have been linearly interpolated at six second intervals, coinciding with every third VLBI residual delay delivered by the correlator

Both plots exhibit strong correlations between the VLBI and WVR time series over the full $\sim$ 2000 second time scale, especially scan 93 which had much larger delay variations. Scan 20 occurred at 9 A.M. local time, before the development of large scale convect ion in the lower troposphere. in contrast, scan 93 occurred at 3 }'. M. local time, near the peak of large scale, turbulent convection.

The rms of the delay variations in Figure 1 arc summarized in 'J'able 1, for the VLBI and WVR data separately and for the differenced time series (not plotted)

$\Delta(t)$ = VLBI(t) - WV R(t). Also shown are estimates of the tropospheric volume sampling error $\sigma_{\rm beam}$ (the expected rms delay difference due to WVR/VLBI antenna beam offset, WVR/VLBI antenna beam mismatch and WVR non-sidereal tracking) and A*, the rms of the differenced time series after subtraction of $\sigma_{\rm beam}$ in quadrature. The method described in [*Linfield and Wilcox,* 1993], scaled by stall-dcpcndcnt estimates of tropospheric activity [*Linfield et al.,* 1996], was used to calculate $\sigma_{\rm beam}$.

For scan 20, the WVR time series had a much larger rms than the VLBI time series. However, the rms of A(t) is smaller than the WVR rms y-3p ps in quadrature, indicating that a 3 ps troposphere variation is common to the VLBI and WVR data, but that the WVR instrumental noise is large compared to the troposphere for this scan. In contrast, the WVR and VLBI time series for scan 93 showed comparable variation and the rms of A(t) is significantly lower than the rms of both the VI .BI and the WVR data, implying that 11-12 ps (rms) of tropospheric delay fluctuations have been removed by the calibration and confirming that the site-diffcrcnccd delay residuals are troposphere dominated. Note that, A* is approximately the same for both scans, suggesting that the noise floor for the VLBI/WVR comparison technique with current instrumentation is $\sim$5-6 ps.

Figure 2 shows the Allan standard deviation of the delay u, (At) as a function of time interval Δt for scan 93 for VLBI, WVR, and their difference $\Delta(t)$. The VLBI and WVR data have similar spectral shapes, except for time scales $\lesssim$ 30 s, where thermal noise, characterized by the much steeper slope of the data, dominates the WV]{ spectrum. For thermal noise $\sigma_\tau(\Delta t) = \sqrt{3}\,N/\Delta t$, where N is the rms of the lloisc-induced delay variations. From Figure 2, $\sigma_\tau(10\ {\rm s}) \sim 7 \times 10^{-13}$ s/s = $7 \times 10^{-12}\,{\rm s}/\Delta t$, implying N $\sim$ 4 ps, approximately the same as A* in "J'able 1. For time intervals > 100 s, the differenced data show less power than either the VLBI or WVR data separately, with the reduction being a factor of $\approx$ 2 for time intervals longer than $\sim$ 200 s. Also shown in Figure 2 is the estimate of σ_τ (At) duc to the tropospheric volume sampling

differences, described above, between the WVR and DSN antennas. For time intervals longer than $\sim$ 200 s, the Allan deviation of A(t) is within a factor of $\approx$ 2 of this estimated error source.

Figure 3 shows the scan-averaged, *zenith* delay residuals of the VLBI and WVR data. The 1,0S residuals $\tau(\theta)$ have been mapped to zenith residuals τ_z to remove variations due solely to elevation angle differences between scans, using the mapping function τ_z = T(U) sin θ. Figure 3(a) shows all 80 scans with *valid* data while Figure 3(b) shows the 30 scan subset for which the WVRs were *co-pointing* with the DSN antennas to better than 10 at both ends of the baseline. The VLBI 1,0S residuals were determined with respect to an *a priori* delay model [*Sovers and Jacobs, 1994]* after the estimation of three parameters from the data: a clock difference τ_{cl}, a clock rate $\dot{\tau}_{cl}$, and a mean zenith troposphere difference $\bar{\tau}_z$. In order to compare the VLBI and WVR time series, the LOS WVR data had an equivalent linear model fitted to ant] subtracted from the data.

A strong correlation between VLBI and WVR estimates of site-diffcrcmccd, residual delays is evident in Figure 3, particularly for the co-pointing data. Because a mean zenith troposphere has been removed, the variations represent the effects of tropospheric fluctuations. The VLBI/WVR correlation shows the ability of WVRs to provide a calibration on time scales ranging from the few minutes between individual scans to $\sim$ 7 hours (half the experiment duration; fluctuations on longer time scales would be absorbed by the fitting).

The WVR estimates of the 1,0S, site-difl'crenccd delay fluctuations can be applied directly as a calibration before parameter estimation. The post-fit rms delay residuals are tabulated in 'J'able 2 for different sets of estimated parameters, both for the full and co-pointing data sets. Results arc given with and without the WVR calibration. Application of the calibration caused a dramatic reduction in the VLBI residuals in all cases. The calibration had the biggest impact when only τ_{cl} and τ_z were estimated, .

as would be expected if the estimated clock rate $\dot{\tau}_{cl}$ also removed part of the linearly varying component of the troposphere. The largest single reduction in rms, a factor of 3.6, occurred when τ_{cl} and τ_z were estimated for the full data set, in spite of a VLBI/WVR angular offset for numerous scans. This is because many low elevation angle scans ($O < 20°$) introduced large tropospheric effects for this data set. When only the 30 scans with co-pointed VLBI and WVR data were included, the reduction in rms residuals was a factor of 2.2--2.6. A significant fraction of the rms delay residual of 16.9 ps for the co-pointing data can be accounted for by the 10.3 ps thermal noise in the VLBI group delay data type and ≈ 2.4 ps from WVR pointing error.

Another possible error source for VLBI/WVR comparisons is *dry* delay fluctuations, duc to temperature fluctuations in the components of dry air, which dominate astronomical "seeing" at optical wavelengths. However, measurements of the outer scale of turbulence in temperature fluctuations [*Barat and Bertin*, 1 984; *Coulman et al.*, 1988] suggest that dry fluctuations will saturate for time scales larger than a few seconds during stable atmospheric conditions (e.g. at night) and for time scales larger than a few hundred seconds during large scale daytime convection. Dry fluctuations may therefore explain part, of the VLBI -- WVR discrepancy within scan 93, but arc probably not an important component of the uncalibrated scan-to-scan residuals shown in Table 2.

Acknowledgments. Wc thank C. Jacobs and C. Naudet for assistance with the experiment scheduling, and L. Skjerve, L. Tanida, R. Swindlehurst and the 1)SS13 crew for assistance with the observations.

References

Barat, Jean, and Bertin, 1'., *Journal of the Atmospheric Sciences, 41*, 819827, 1984.

Coulman, C. E., Vernin, J., Coqueugniot, Y., and Caccia, J. L., *Applied optics)* 27, 155--160, 1988.

Elgered, G., *in Atmospheric Remote Sensing by Microwave Radiometry*, chap. 5, edited by M. Janssen, John Wiley, New York, 1993.

Hinder, R. A., *Nature,* 225, 614-617, 1970.

Janssen, M. A., IEEE *Trans. Geosci. Remote Sensing,* 23, 485 490, 1985.

Keihm, S. J., *JPL Doc. D-8898,* Jet Propul. Lab., Pasadena, CA., 1991.

Linfield, R.P., and Wilcox, J. Z., *The Telecommunications and Data Acquisition Progress Report, JPL Rep. 42-114, 1-9,* Jet Propul. Lab., Pasadena, CA, 1993.

Linfield, R.P., Keihm, S. J., Teitelbaum, 1,.1'., Walter, S. J., Mahoney, M. J., Treuhaft, R. N., and Skjerve, L. J., *Radio Science, 31, 129-* 146, 1996.

Lowe, S.T., *Theory of Post-Block II VLBI Observable Extraction*, JPL publication 92-7, Jet Propul. Lab., Pasadena, CA, 1992.

O.J. Sovers, O. J., and Jacobs, C. S., *Observation Model and Parameter Partials for the JPI, VLBI Paramet - Estimation Software "MODEST" - 1994,* J] 'I, publication 83-38, ": / Rev. 5, Jet Propul. Lab., Pasadena, CA, 1994.

Treuhaft, R.N., and Lanyi, G. E., *Radio Science,* 22, 251-265, 1987

This manuscript was prepared with the AGU LaTeX macros v3. 1.

Figure 1. Site-diffcrcncccl, line-of-siglkt (LOS) delay residuals for two long scans. Both the VLBI and WVR delays arc residuals with respect to linear fits (see text).

Figure 2. Allan standard deviation σ_τ (At) of VLBI, WVR and VLBI-WVR delay residuals for scan 93. The solid line is an estimate of the σ_τ (At) introduced because the VLBI and WVR antennas sampled different tropospheric volumes.

Figure 3. Site- differenced *zenith* delay residuals for scan-averaged VLBI and WVR data. Note the difference in time scale compared to Figure 1. The top plot shows all 80 valid scans while the bottom plot shows only those 30 scans where the VLBI and WVR were co-pointing.

'J'able 1. RMS (ps) of the delay variations of Figure 1. Also shown are the RMS of the differenced time series A (t), the tropospheric volume sampling error σ_{beam}, and A", the RMS of the differenced time series after subtracting σ_{beam} in quadrature.

Scan	VLBI (t)	WVR(t)	$A(t)$	σ_{beam}	A"
20	3.54	6.04	5.08	1.0	5.0
93	13.7	13.9	7.56	4.8	5.8

Table 2. RMS of the post-fit delay residuals after parameter estimation (ps).

	Valid (80 scans)		Co-pointing (30 scans)	
Estimated parameters	No WVR	WVR	No WVR	WVR
$\tau_{\text{cl}}, \dot{\tau}_{\text{cl}}, \tilde{\tau}_z$	106	52.0	43.8	16.9
$\tau_{\text{cl}}, \dot{\tau}_{\text{cl}}$	139	85.4	47.5	22.0
$\tau_{\text{cl}}, \tilde{\tau}_z$	193	53.2	102	38.7
τ_{cl}	220	92.3	102	38.7

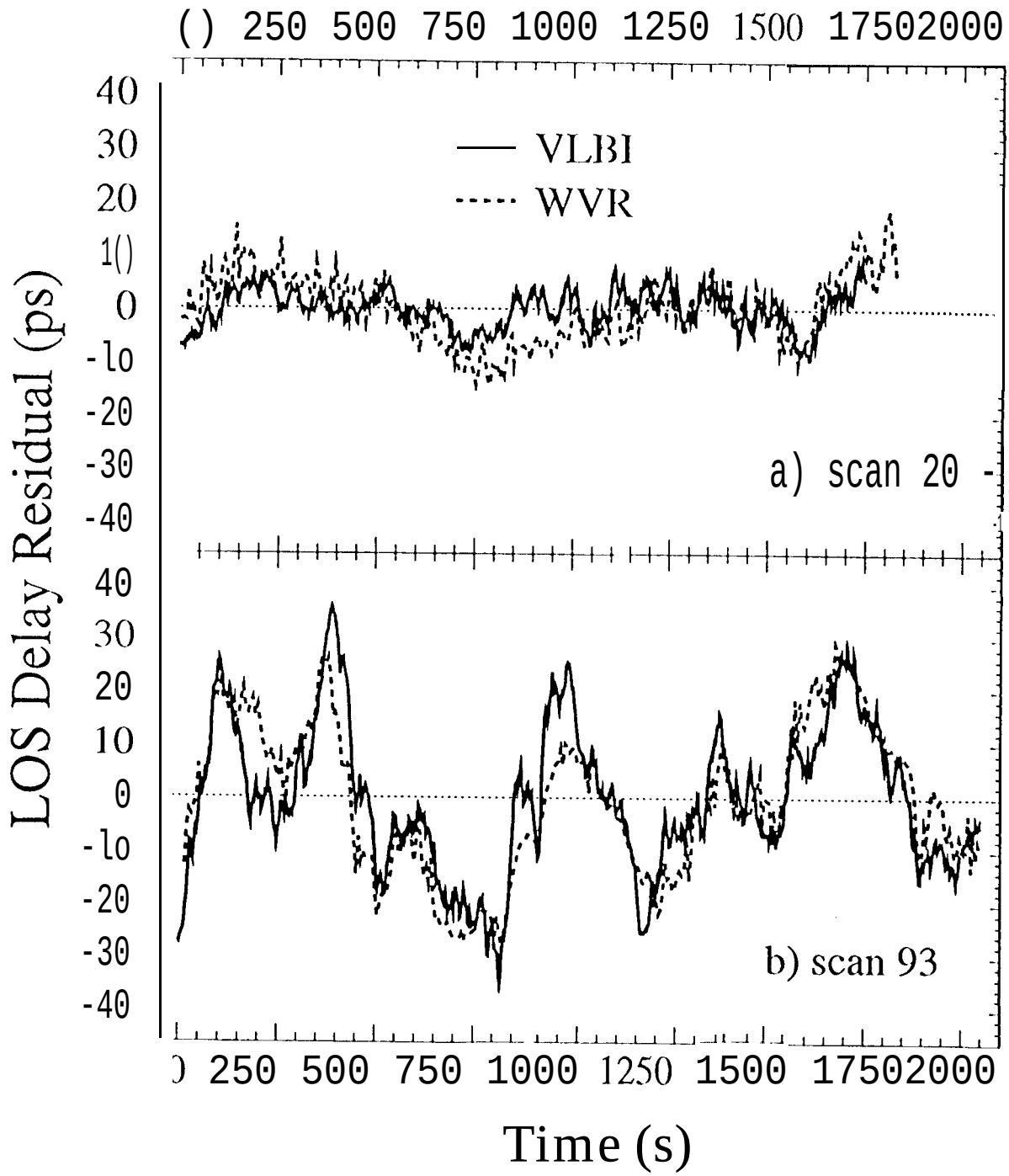
( ) 250 500 750 1000 1250 1500 17502000
40
30
20
1()
0
-lo
-20
-30
-40
VLBI
WVR
a) scan 20 -
40
30
20
10
0
-lo
-20
-30
-40
b) scan 93
) 250 500 750 1000 1250 1500 17502000
LOS Delay Residual (ps)
Time (s)

Figure 1

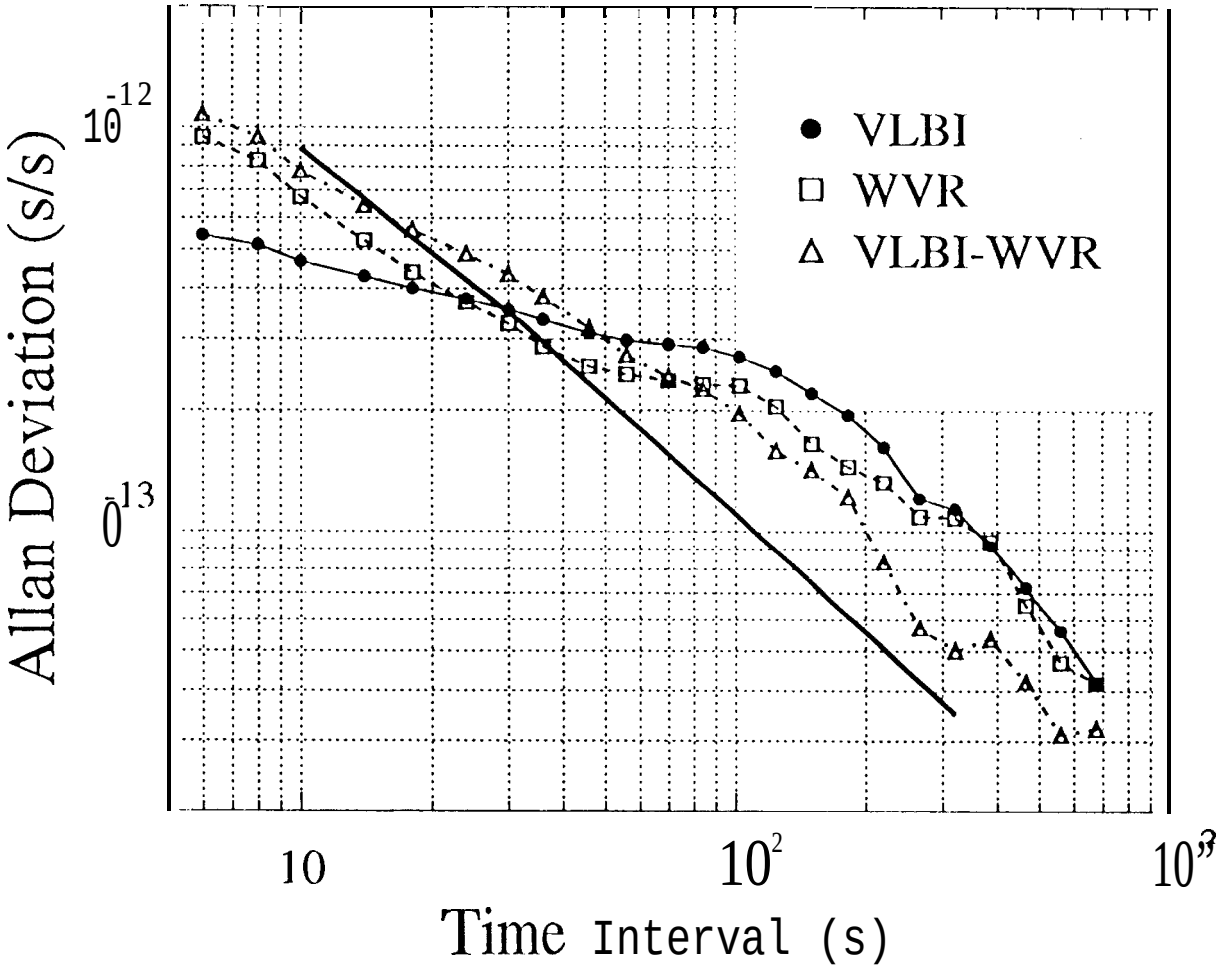
Allan Deviation (s/s)
10^-12
10^-13
VLBI
WVR
VLBI-WVR
10
10^2
10^3
Time Interval (s)

Figure 2

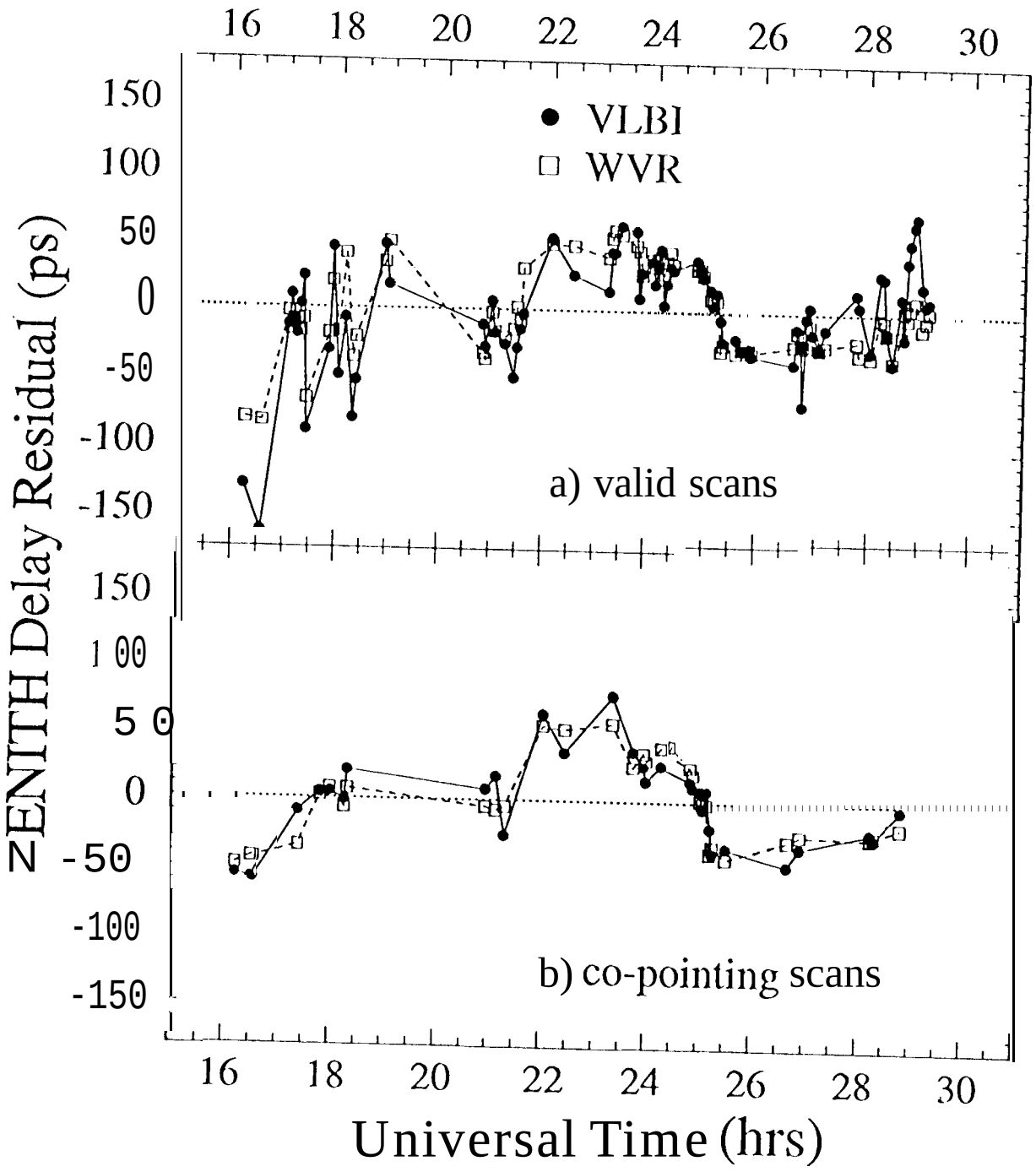
16
18
20
22
24
26
28
30
150
100
50
0
-50
-100
-150
VLBI
WVR
a) valid scans
b) co-pointing scans
ZENITH Delay Residual (ps)
Universal Time (hrs)

Figure 3